Experimental and Molecular Pathology 144 (2025) 105005

Contents lists available at ScienceDirect

Experimental and Molecular Pathology

journal homepage: www.elsevier.com/locate/yexmp

High *KCNJ14* expression is associated with an immunosuppressive tumor microenvironment and advanced pathological features: An RNA in situ hybridization-based analysis of colorectal carcinoma

Hiroshi Sawaguchi [a], Takeshi Uehara [b,*], Mai Iwaya [b], Shiho Asaka [b,c], Tomoyuki Nakajima [b], Shotaro Komamura [b], Shunsuke Imamura [a], Yugo Iwaya [a], Shinsuke Sugenoya [d], Masato Kitazawa [d], Yuji Soejima [d], Hiroyoshi Ota [b,e], Tadanobu Nagaya [a]

[a] Division of Gastroenterology and Hepatology, Department of Medicine, Shinshu University School of Medicine, Matsumoto, Japan
[b] Department of Laboratory Medicine, Shinshu University School of Medicine, Matsumoto, Japan
[c] Department of Laboratory Medicine and Pathology, Life Science Research Center, Nagano Children's Hospital, Azumino, Japan
[d] Division of Gastroenterological, Hepato-Biliary-Pancreatic, Transplantation and Pediatric Surgery, Department of Surgery, Shinshu University School of Medicine, Matsumoto, Japan
[e] Department of Clinical Laboratory Sciences, Shinshu University School of Medicine, Matsumoto, Japan

ARTICLE INFO

Keywords:
KCNJ14
Colorectal carcinoma
Tumor microenvironment

ABSTRACT

Colorectal carcinoma (CRC) remains one of the leading causes of cancer-related deaths worldwide, and there is a lack of reliable biomarkers to predict tumor progression and the immune microenvironment. *KCNJ14* is a member of the inwardly rectifying potassium channel family that has recently been implicated in tumor progression and immune suppression; however, its clinical significance and spatial expression patterns in CRC remain unclear. We evaluated *KCNJ14* mRNA expression by RNA in situ hybridization using an RNAscope on a tissue microarray of 259 CRC cases. We assessed the associations between *KCNJ14* expression and clinicopathological features, tumor-infiltrating $CD4^+$, $CD8^+$, and $FOXP3^+$ cells, and patient outcomes. We also performed single-cell RNA sequencing analysis to determine the cell type-specific expression of *KCNJ14*. *KCNJ14* expression was predominantly observed in cancer cells, with high expression identified in 36 cases. High *KCNJ14* expression was significantly associated with lymphatic invasion, venous invasion, lymph node metastasis, and advanced disease stage. High *KCNJ14* expression was also correlated with decreased intratumoral infiltration of $CD4^+$ and $CD8^+$ T cells, as well as lower tumor-infiltrating lymphocyte scores, indicating an immunosuppressive tumor microenvironment. In contrast, there were no significant associations between *KCNJ14* expression and $FOXP3^+$ cell infiltration, overall survival, or recurrence-free survival. This study is the first to demonstrate that high *KCNJ14* expression is associated with an immunosuppressive tumor microenvironment and advanced pathological features in CRC. Although *KCNJ14* is not an independent prognostic factor, it may serve as a potential indicator of an immunosuppressive tumor microenvironment and be a novel therapeutic target.

1. Introduction

Colorectal carcinoma (CRC) is one of the most prevalent gastrointestinal malignancies worldwide and is a major cause of cancer-related mortality (Bray et al., 2024; Arnold et al., 2017). The survival of patients with CRC has been improved by advances in surgical techniques, chemotherapy, molecular targeted therapy, and immunotherapy, even in advanced cases. However, the prognosis remains poor for many patients with CRC, particularly those with recurrence or metastasis, and the outcomes vary considerably between individuals. In the United States, CRC is the second leading cause of cancer-related death after lung cancer (Siegel et al., 2024). Furthermore, CRC is the leading cause of cancer death among men and the second leading cause of cancer death among women under the age of 50 years, indicating a high burden of disease in young adults (Siegel et al., 2024). These facts underscore the urgent need to identify novel molecular biomarkers beyond conventional staging systems that are capable of predicting the prognosis of patients with CRC (Bray et al., 2024).

* Corresponding author at: Department of Laboratory Medicine, Shinshu University School of Medicine, 3-1-1 Asahi, Matsumoto, Nagano 390-8621, Japan.
E-mail address: tuehara@shinshu-u.ac.jp (T. Uehara).

https://doi.org/10.1016/j.yexmp.2025.105005
Received 10 August 2025; Received in revised form 16 October 2025; Accepted 17 October 2025
Available online 21 October 2025
0014-4800/© 2025 The Authors. Published by Elsevier Inc. This is an open access article under the CC BY-NC-ND license (http://creativecommons.org/licenses/by-nc-nd/4.0/).

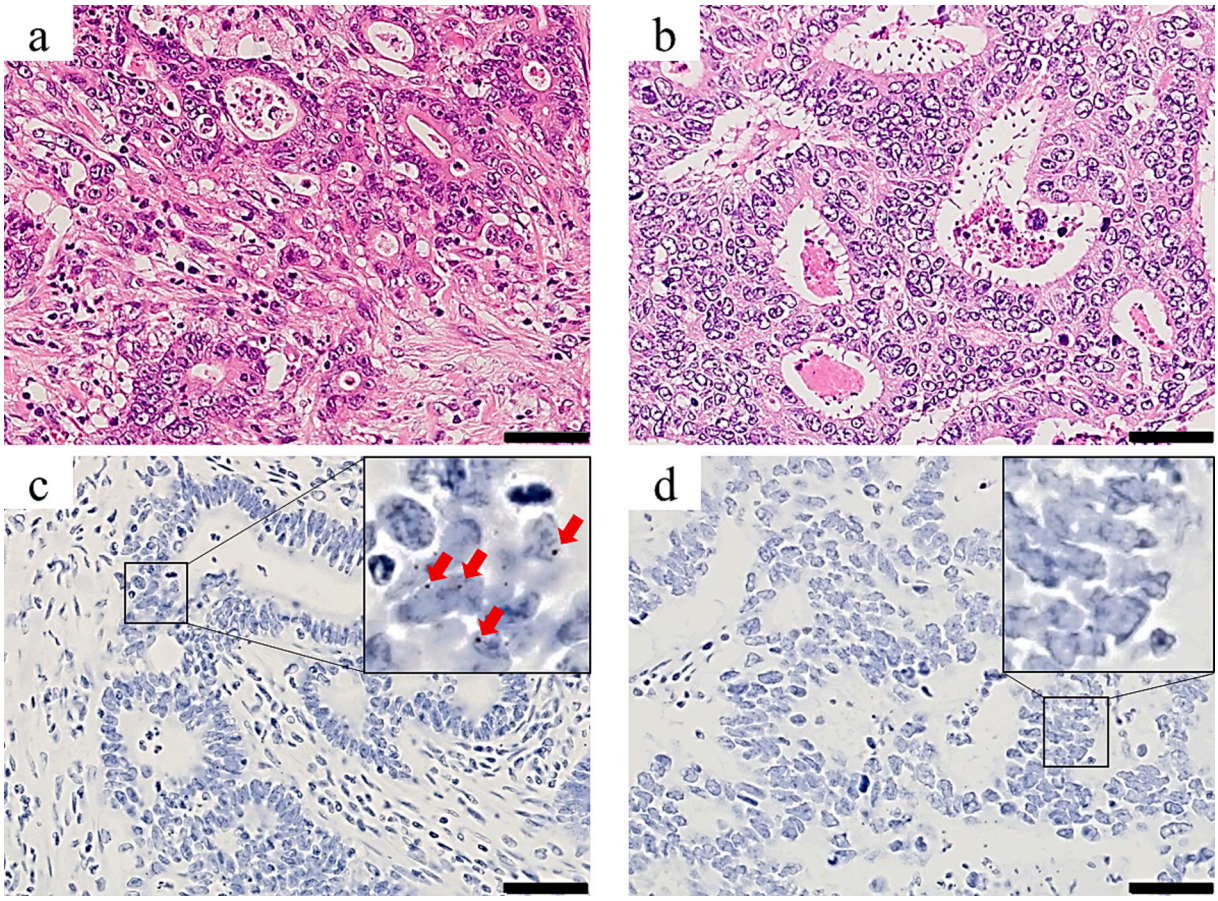

Fig. 1. RNA-ISH and H&E staining of *KCNJ14* expression in colorectal cancer.
Hematoxylin and eosin (H&E) staining in representative cases of (a) high and (b) low *KCNJ14* expression. (c, d) RNAscope images from the corresponding cases. (c) In cases with high *KCNJ14* expression, brown punctate signals indicating *KCNJ14* mRNA are visible in tumor cells. (d) In cases with low *KCNJ14* expression, such signals are scarcely observed. Scale bar = 50 μm. (For interpretation of the references to colour in this figure legend, the reader is referred to the web version of this article.)

In CRC, the prognosis and treatment response have been linked to genetic alterations such as KRAS, BRAF, and PIK3CA mutations, as well as microsatellite instability. However, there are still limited universally applicable prognostic indicators for the broader population of patients with CRC (Dienstmann et al., 2017). In this context, ion channels—particularly potassium channels located on the cell membrane—have recently gained attention. These ion channels not only regulate membrane potential and ion homeostasis, but are also increasingly being recognized as key factors in tumor biology that contribute to cancer cell proliferation, migration, invasion, and metabolism (Hernandez-Resendiz et al., 2019; Pardo and Stuhmer, 2014).

The *KCNJ14* gene (also known as Kir2.4) encodes an inwardly rectifying potassium channel and belongs to the Kir channel family, which comprises 15 genes classified into seven subfamilies (Kir1.x to Kir7.x) (Zhang et al., 2021). Recent studies have reported that *KCNJ14* is overexpressed in various malignancies, particularly gastrointestinal cancers, and is associated with tumor progression (Zuniga et al., 2022). *KCNJ14* is located on chromosome 19q13 and encodes a protein that has been linked to numerous biological functions, including heart rate regulation, neurotransmitter release, and immune modulation (Topert et al., 2000; Hazra et al., 2011; Topert et al., 1998; Chiang et al., 2020).

Comprehensive analyses of large-scale databases such as the Cancer Genome Atlas and the Gene Expression Omnibus have revealed that *KCNJ14* is highly expressed in CRC and is correlated with advanced tumor stage, activation of the mechanistic target of rapamycin (mTOR) signaling pathway, and an immunosuppressive tumor microenvironment (TME) (Jin et al., 2025; Alasiri, 2023; Li et al., 2022). These findings suggest that *KCNJ14* may be involved not only in tumor-intrinsic signaling but also in the negative regulation of immune responses, thus representing a potential prognostic biomarker and therapeutic target.

Most research on the role of *KCNJ14* in CRC has relied primarily on RNA sequencing or in silico bioinformatics analyses. To date, no studies have directly visualized the spatial and cellular expression patterns of *KCNJ14* in CRC while preserving tissue architecture. RNA in situ hybridization (RNA-ISH) is a highly sensitive and specific technique for detecting mRNA expression at the cellular level in formalin-fixed paraffin-embedded samples. The RNAscope method enables the quantitative and visual assessment of tumor-specific mRNA expression within intact tissue architecture and is particularly well suited to molecular pathological diagnostics due to its reproducibility and reliability (Wang et al., 2012).

Clarifying the extent and localization of *KCNJ14* expression at the mRNA level in CRC tumor cells, and investigating its association with clinicopathological features and outcomes using actual patient specimens, may provide valuable insights for future diagnostic and therapeutic strategies. In the present study, we performed RNA-ISH using an RNAscope on a CRC tissue microarray (TMA) to histologically characterize *KCNJ14* expression patterns and evaluate their clinical significance.

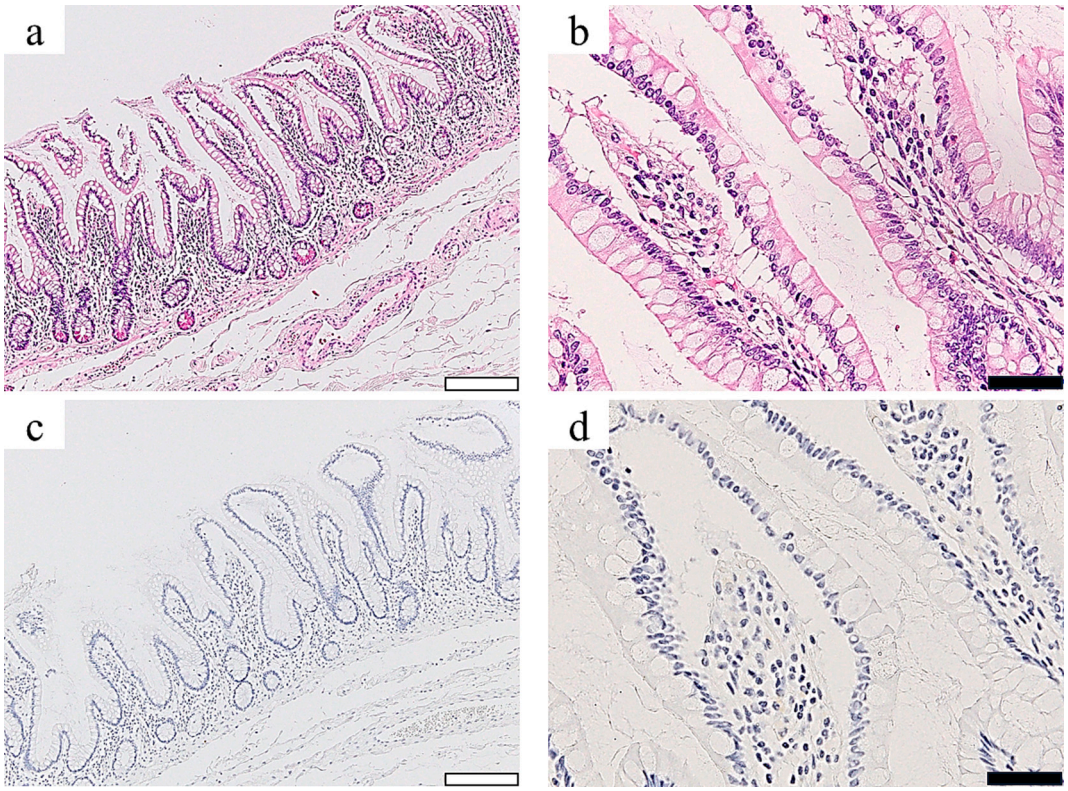

Fig. 2. *KCNJ14* expression in normal colorectal mucosa.
Representative images of normal colorectal mucosa with hematoxylin and eosin staining (a, b) and *KCNJ14* RNA in situ hybridization (c, d). No detectable *KCNJ14* expression was observed in normal colorectal epithelium. White scale bars = 200 μm; black scale bars = 50 μm.

2. Materials and methods

2.1. Patients

This study included 305 patients who underwent surgical treatment of CRC at Shinshu University Hospital between 2014 and 2022. All patients were monitored for a minimum follow-up period of 2 years. Adenocarcinomas were categorized as well-differentiated, moderately differentiated, or poorly differentiated. Based on previously published criteria (Fleming et al., 2012), well-differentiated and moderately differentiated adenocarcinomas were classified as low grade, whereas poorly differentiated adenocarcinomas were classified as high grade. Of these 305 patients, 46 were excluded for the following reasons: 40 were negative for the positive control (housekeeping gene) in the TMA, and six had no tumor tissue at the primary site within a TMA. Ultimately, 259 patients with CRC were analyzed.

Clinical and pathological data, including patient age, sex, tumor differentiation, outcomes, lymph node involvement, vascular invasion, tumor-infiltrating lymphocytes (TILs), TNM classification, and location (proximal, distal, rectal), were extracted from medical records. Tumor staging and differentiation were defined in accordance with the eighth edition of the Union for International Cancer Control classification (Brierley and Wittekind, 2017) and the fifth edition of the World Health Organization classification (Nagtegaal and Lam, 2020). Histological evaluation of all specimens was independently performed by two pathologists (TU and MI). TILs in tumor-infiltrating regions were scored using a four-tier system as 0 (none), 1 (mild), 2 (moderate), or 3 (marked) (Ropponen et al., 1997). For subsequent analyses, the TIL scores were categorized as low (scores 0 and 1) or high (score 2 and 3).

Overall survival (OS) was defined as the duration between the date of surgical resection and either death or last follow-up. Recurrence-free survival (RFS) was defined as the time from surgical resection to disease recurrence or the last follow-up without recurrence. This study adhered to the ethical principles outlined in the Declaration of Helsinki and received approval from the Clinical Trial Review Committee of Shinshu University School of Medicine (approval number: 5836).

2.2. Histopathology and tissue microarray construction

All specimens were fixed in 10 % or 20 % neutral-buffered formalin and embedded in paraffin. For the construction of a TMA, blocks containing sufficient tumor tissue from the invasive frontline were selected from the formalin-fixed paraffin-embedded archives. Tissue cores (3-mm in diameter) were punched out from each block using thin-walled stainless steel needles (Azumaya Medical Instruments Inc., Tokyo, Japan) and arrayed into a recipient paraffin block. Serial 4-μm-thick sections were cut from the TMA blocks. One section from each TMA was stained with hematoxylin and eosin for histological assessment.

2.3. Immunohistochemical analysis and evaluation

To evaluate subsets of tumor-infiltrating lymphocytes, IHC staining for CD4, CD8, and FOXP3 was performed on serial TMA sections using a fully automated staining system (BOND-III; Leica Biosystems, UK). The following primary antibodies were used: CD4 (clone 4B12, ready-to-use; Leica Biosystems), CD8 (clone C8/144B, ready-to-use; Leica Biosystems), and FOXP3 (clone 236 A/E7, 1:100 dilution; Abcam, UK).

For evaluation, three areas with the highest density of $CD4^+$, $CD8^+$, or $FOXP3^+$ cells were selected from each core. Cell counts per high-powered field (HPF; 10× ocular, 40× objective; area of 0.345 mm^2) were performed directly under a microscope. The average cell count of the three fields was used for analysis, and the median of these counts was used as the cutoff to classify cases into low and high infiltration groups.

Additionally, the TMA was subjected to immunohistochemical staining for mismatch repair proteins (MMR), including MLH1 (clone ES05, mouse monoclonal, 1:50), PMS2 (clone EP51, rabbit monoclonal,

Table 1
KCNJ14 expression and clinicopathological characteristics in CRC.

		KCNJ14 expression		
Factors	$n = 259$	Low ($n = 223$)	High ($n = 36$)	*P*-value
Age				0.367
<70 years	116	97	19	
≥ 70 years	143	126	17	
Sex				0.072
Male	151	125	26	
Female	108	98	10	
Histological grade				0.188
Low	224	190	34	
High	35	33	2	
Lymphatic invasion				**0.004**
Present	129	103	26	
Absent	130	120	10	
Venous invasion				**p < 0.001**
Present	186	152	34	
Absent	73	71	2	
Location				0.13
Proximal	72	63	9	
Distal	78	62	16	
Rectal	109	98	11	
MSI				1
dMMR	23	20	3	
pMMR	232	199	33	
TIL				**0.019**
High	129	118	11	
Low	130	105	25	
CD4				**0.003**
High	115	107	8	
Low	130	104	26	
CD8				**p < 0.001**
High	127	120	7	
Low	126	97	29	
FOXP3				0.474
High	128	112	16	
Low	125	105	20	
LN metastasis				**p < 0.001**
Present	123	92	31	
Absent	136	131	5	
TNM stage				**p < 0.001**
0-II	130	127	3	
III-IV	129	96	33	

LN, lymph node

1:40), MSH2 (clone FE11, mouse monoclonal, 1:50), and MSH6 (clone EP49, rabbit monoclonal, 1:50; Agilent Technologies, Santa Clara, CA, USA), using validated protocols (Nakajima et al., 2020). MMR protein deficiency was defined as the absence of expression of at least one of the four markers. A specimen was considered MMR-deficient if any of the four MMR proteins showed a complete lack of immunoreactivity. All histological features and staining results were independently evaluated by two experienced pathologists (TU and MI).

2.4. *KCNJ14* analysis by RNA in situ hybridization

Detection of *KCNJ14* mRNA on unstained sample tissue slides was performed using an RNAscope kit (Advanced Cell Diagnostics, Hayward, CA, USA) in accordance with the manufacturer's instructions. The detailed procedure is described in a previous report (Ukpo et al., 2011). Briefly, tissue sections were pretreated with heating and protease application prior to hybridization with a *KCNJ14*-specific probe. Positive staining was indicated by brown punctate dots in the nucleus and/or cytoplasm. Standard Mm-PPIB (ACD-313902) was used as a positive control to ensure interpretable results. *KCNJ14* expression was quantified using the five-grade scoring system recommended by the manufacturer in which 0 indicates no staining, 1+ indicates 1–3 dots/cell, 2+ indicates 4–9 dots/cell, 3+ indicates 10–15 dots/cell and/or < 10 % dots are in clusters, and 4+ indicates >15 dots/cell and/or > 10 % dots are in clusters, under a 40× objective lens (Olympus BX53). The *KCNJ14* mRNA expression was then categorized as low (grades 0 and 1+) or high (grades 2+, 3+, and 4+). We analyzed the relationship between *KCNJ14* expression and clinicopathological data and outcomes in patients with CRC.

2.5. Single-cell RNA sequencing analysis of *KCNJ14* expression in colorectal carcinoma

Single-cell RNA sequencing (scRNA-seq) analysis of *KCNJ14* expression was conducted using the publicly available dataset (accession number: GSE132465) obtained from the NCBI Gene Expression Omnibus database. This dataset comprised 23 tumor samples and 10 normal samples derived from CRC tissues. Data processing and analysis were conducted using the Seurat R package (v4.1.0). Raw count matrices were normalized to a total expression of 10,000 molecules per cell and subsequently scaled. Highly variable genes across cells were identified and used for principal component analysis to reduce dimensionality. The FindNeighbors and FindClusters functions were used to assess cellular similarities and perform clustering. Visualization of cellular heterogeneity was achieved by applying uniform manifold approximation and projection using the runUMAP function. The expression distribution of *KCNJ14* marker genes was assessed across the clusters, allowing for cell type annotation.

2.6. Statistical analysis

Categorical variables were expressed as frequencies, and differences between subgroups were assessed using Fisher's exact test. The Mann–Whitney *U* test was used to compare immune cell infiltration levels ($CD4^+$, $CD8^+$, and $FOXP3^+$ cells) between the high *KCNJ14* expression and low *KCNJ14* expression groups. To visualize the distribution of immune cell counts, violin plots were generated using the ggplot2 package in R. OS and RFS were estimated by the Kaplan–Meier method, and between-group comparisons were performed using the log-rank test. Univariate Cox proportional hazards regression analysis was also performed to evaluate the association between *KCNJ14* expression and patient prognosis (OS and RFS).

Statistical significance was defined as $P < 0.05$. All statistical analyses were performed using EZR (Easy R), version 1.66, a graphical interface for R developed by the R Foundation for Statistical Computing (Vienna, Austria).

3. Results

3.1. High KCNJ14 expression correlates with advanced pathological features and an immunosuppressive tumor microenvironment

Positive *KCNJ14* signals were observed as brown punctate dots in the nucleus and cytoplasm of cancer cells (Fig. 1a, c). Some cases had no positive dots (Fig. 1b, d). Among the 259 CRC cases, 115 showed

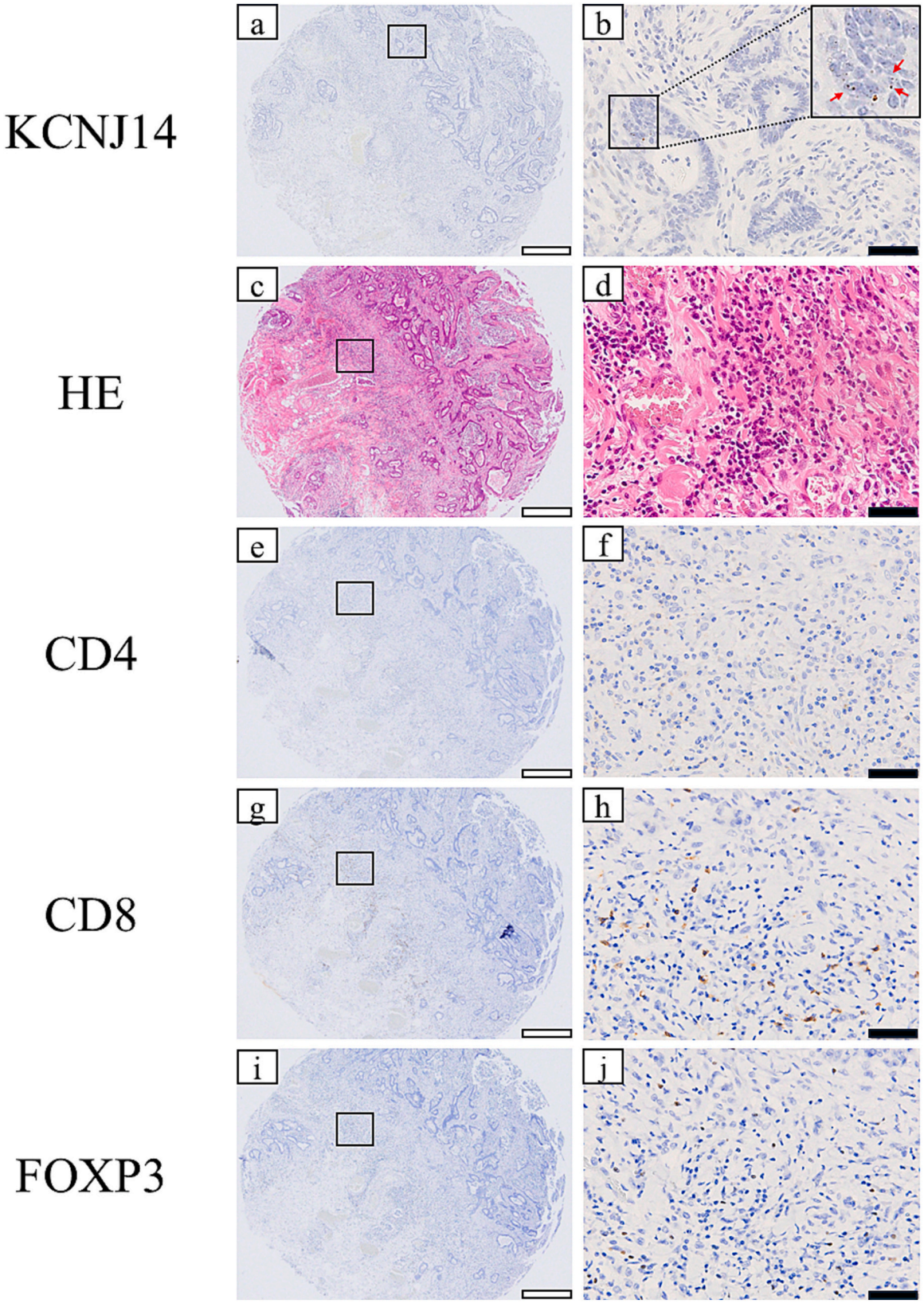

Fig. 3. Representative case with high *KCNJ14* expression and low TIL infiltration.
Representative images from a colorectal carcinoma case with high *KCNJ14* expression. RNA-ISH for *KCNJ14* (a, b), hematoxylin and eosin staining (c, d), and serial sections stained for CD4 (e, f), CD8 (g, h), and FOXP3 (i, j) are shown. The tumor shows strong *KCNJ14* expression with low infiltration of $CD4^+$, $CD8^+$, and $FOXP3^+$ cells. White scale bars = 500 μm; black scale bars = 50 μm.

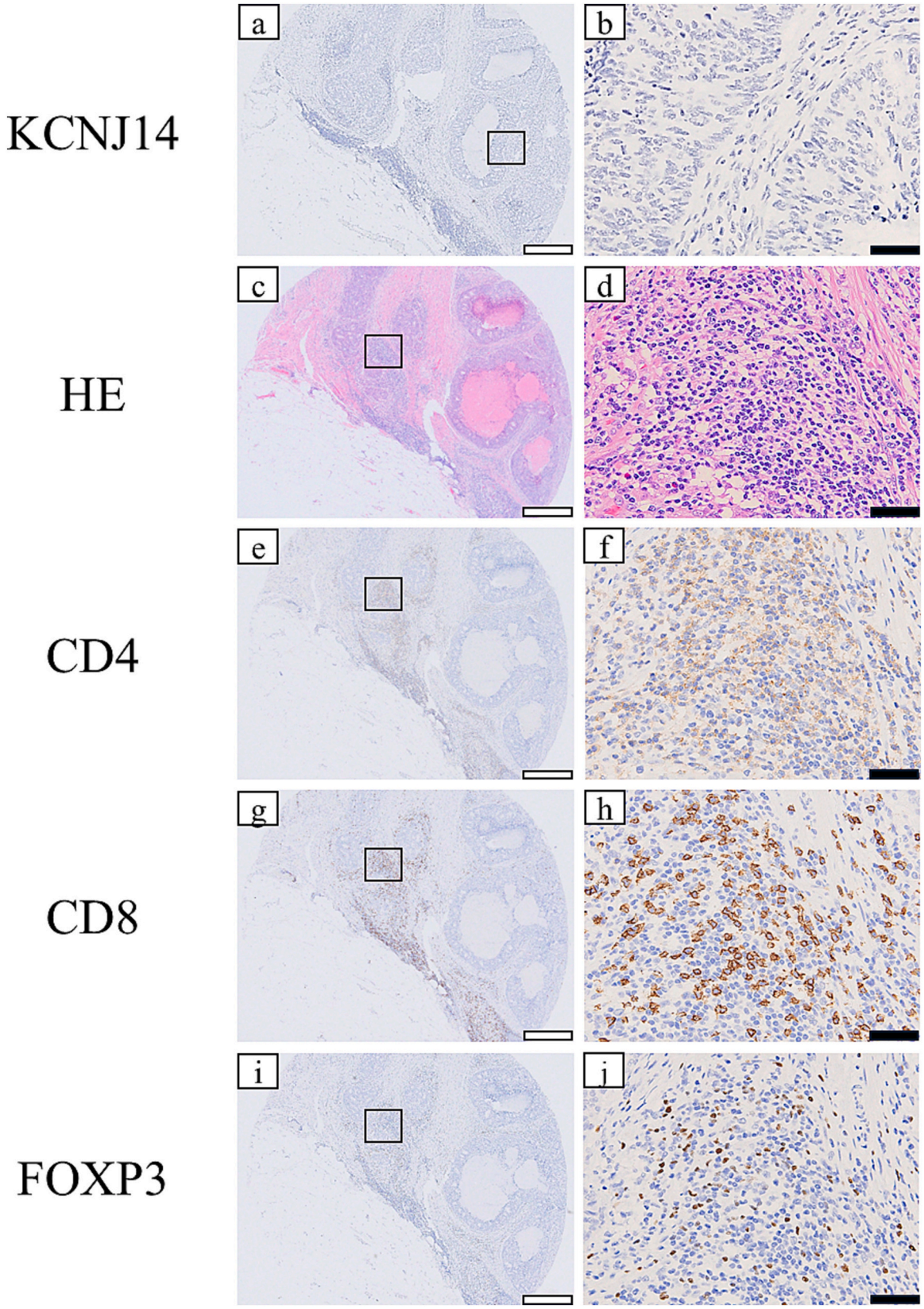

Fig. 4. Representative case with low *KCNJ14* expression and high TIL infiltration.
Representative images from a colorectal carcinoma case with low *KCNJ14* expression. RNA-ISH for *KCNJ14* (a, b), hematoxylin and eosin staining (c, d), and serial sections stained for CD4 (e, f), CD8 (g, h), and FOXP3 (i, j) are shown. The tumor shows weak *KCNJ14* expression with high infiltration of $CD4^+$, $CD8^+$, and $FOXP3^+$ cells. White scale bars = 500 μm; black scale bars = 50 μm.

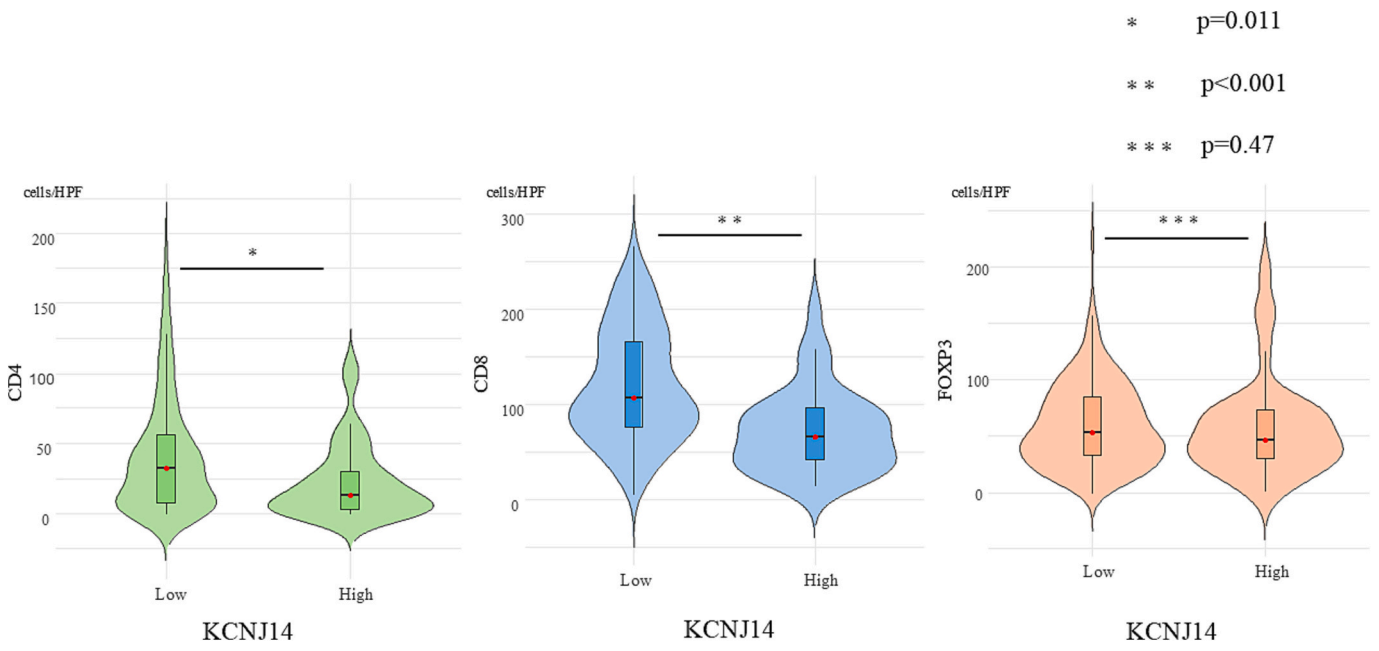

Fig. 5. Association between *KCNJ14* expression and the tumor immune microenvironment.
Violin plots showing the distribution of tumor-infiltrating T cells ($CD4^+$, $CD8^+$, and $FOXP3^+$) in groups with high and low *KCNJ14* expression. Mann–Whitney *U* tests reveal significantly lower infiltrations of $CD4^+$ ($p = 0.011$) and $CD8^+$ ($p < 0.001$) T cells in the high *KCNJ14* expression group, but no significant intergroup difference in $FOXP3^+$ cells ($p = 0.47$).

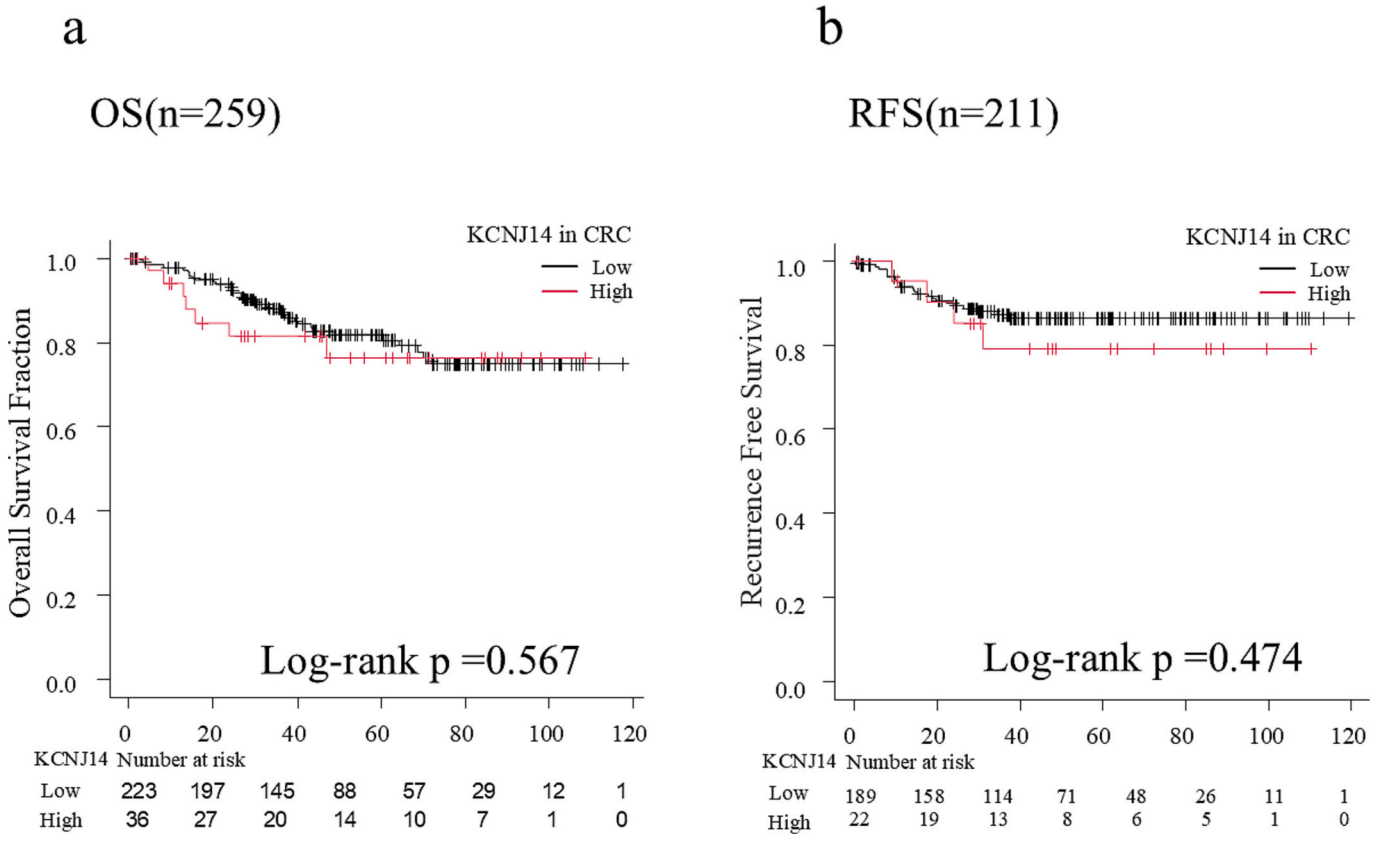

Fig. 6. Kaplan–Meier survival analysis stratified by *KCNJ14* expression
The log-rank test reveal no significant differences between the high *KCNJ14* expression and low *KCNJ14* expression groups in OS ($p = 0.567$) or RFS ($p = 0.474$).

detectable *KCNJ14* dots and 36 were classified as having high *KCNJ14* expression (grade 2+ or higher). However, no *KCNJ14*-positive signals were detected in normal colonic mucosa (Fig. 2).

Compared with the low *KCNJ14* expression group, the high *KCNJ14* expression group exhibited significantly higher frequencies of lymphatic invasion ($p = 0.004$), venous invasion ($p < 0.001$), lymph node

Table 2
Univariate analyses of overall survival factors in CRC.

Factors	Univariate analysis				
	HR	95 %CI			P-value
Age: ≧70 years vs. <70 years	0.95	0.52	–	1.71	0.852
Sex: male vs. female	1.2	0.67	–	2.18	0.531
Histological grade: low vs. high	2.35	1.06	–	5.18	**0.034**
Lymphatic invasion: absent vs. present	3.73	1.84	–	7.54	**p < 0.001**
Venous invasion: absent vs. present	2.14	0.95	–	4.79	0.066
TIL low vs. high	0.28	0.14	–	0.58	**p < 0.001**
CD4 low vs. high	0.72	0.38	–	1.35	0.305
CD8 low vs. high	0.62	0.33	–	1.16	0.132
FOXP3 low vs. high	0.27	0.13	–	0.54	**p < 0.001**
LN metastasis: absent vs. present	2.99	1.54	–	5.8	**0.001**
TNM stage: 0-II vs. III-IV	3.46	1.71	–	7.01	**p < 0.001**
KCNJ14 expression: low vs. high	1.27	0.56	–	2.84	0.568

LN, lymph node.

Table 3
Univariate analyses of recurrence-free survival factors in CRC.

Factors	Univariate analysis				
	HR	95 %CI			P-value
Age: ≧70 years vs. <70 years	1.25	0.57	–	2.73	0.575
Sex: male vs. female	1.32	0.62	–	2.82	0.468
Histological grade: low vs. high	1.42	0.49	–	4.14	0.516
Lymphatic invasion: absent vs. present	2.81	1.26	–	6.25	**0.012**
Venous invasion: absent vs. present	1.8	0.73	–	4.46	0.205
TIL low vs. high	0.82	0.39	–	1.75	0.614
CD4 low vs. high	1.31	0.6	–	2.89	0.5
CD8 low vs. high	1.02	0.47	–	2.20	0.962
FOXP3 low vs. high	0.99	0.46	–	2.16	0.984
TNM stage: 0-II vs. III	4.88	2.06	–	11.55	**p < 0.001**
KCNJ14 expression: low vs. high	1.47	0.51		4.25	0.477

LN, lymph node.

metastasis ($p < 0.001$), and advanced tumor stages III–IV ($p < 0.001$). In addition, compared with the low *KCNJ14* expression group, the high *KCNJ14* expression group had significantly lower TIL scores ($p = 0.019$) and significantly reduced infiltrations of $CD4^+$ T cells ($p = 0.003$) and $CD8^+$ T cells ($p < 0.001$) (Table 1). Representative images illustrating the scoring of $CD4^+$, $CD8^+$, and $FOXP3^+$ cells in relation to *KCNJ14* expression are shown in Fig. 3 and Fig. 4.

The relationship between the abundance of $CD4^+$, $CD8^+$, and $FOXP3^+$ cells and the *KCNJ14* expression level was further analyzed using the Mann–Whitney *U* test (Fig. 5). Both $CD4^+$ and $CD8^+$ T cells were significantly reduced in the high *KCNJ14* expression group (CD4: $p = 0.011$; CD8: $p < 0.001$), while the abundance of $FOXP3^+$ cells did not significantly differ between the low and high *KCNJ14* expression groups ($p = 0.47$).

3.2. *KCNJ14* expression shows no significant impact on overall survival or recurrence-free survival

The prognostic value of *KCNJ14* expression in CRC was evaluated using Kaplan–Meier survival curves and log-rank tests. The median OS of the entire cohort was 39.9 months (95 % CI: 27.6–66.7 months). The median OS was 45.6 months (95 % CI: 16.9–66.4 months) in the high *KCNJ14* expression group and 39.4 months (95 % CI: 28.1–67.4 months) in the low-expression group; however, the intergroup difference was not statistically significant (log-rank test, $p = 0.567$) (Fig. 6a).

For patients with stages I–III CRC ($n = 211$), the median RFS was 38.4 months (95 % CI: 26.9–67.4 months). The median RFS was 45.9 months (95 % CI: 27.7–69.1 months) in the high *KCNJ14* expression group and 38.1 months (95 % CI: 26.9–66.5 months) in the low *KCNJ14* expression group, with no significant difference between the groups (log-rank test, $p = 0.474$) (Fig. 6b).

Consistent with these findings, univariate Cox proportional hazards regression analysis also showed no significant association between *KCNJ14* expression and either OS (HR = 1.27, 95 % CI: 0.56–2.84, $p = 0.568$) or RFS (HR = 1.47, 95 % CI: 0.51–4.25, $p = 0.477$) (Tables 2, 3).

3.3. *KCNJ14* is predominantly expressed in epithelial tumor cell clusters according to single-cell RNA sequencing analysis

scRNA-seq analysis using publicly available data revealed that *KCNJ14* was predominantly expressed in epithelial cell clusters within tumor tissues. In contrast, there was minimal or absent *KCNJ14* expression in immune and stromal cells, including T cells, B cells, mast cells, myeloid cells, and stromal cells (Fig. 7). In normal tissues, *KCNJ14* expression was generally very low and limited to sporadic and low-level expression in epithelial cell clusters.

4. Discussion

In this study, we used RNAscope-based mRNA analysis to investigate the relationship between *KCNJ14* expression and the TME and pathological features in CRC. High *KCNJ14* expression was significantly associated with increased lymphatic invasion, venous invasion, and lymph node metastasis, as well as a higher proportion of advanced-stage tumors, suggesting a potential role in tumor progression.

From an immunological perspective, tumors with high *KCNJ14* expression showed significantly decreased intratumoral infiltration of $CD4^+$ and $CD8^+$ T cells and lower TIL scores, indicating suppressed immune activation within the tumor and the establishment of an "immune-cold" TME (Liu et al., 2023; Wu et al., 2024). These findings support the notion that *KCNJ14* may contribute to the development of an immunosuppressive TME, which is consistent with previous reports (Alasiri, 2023; Li et al., 2022).

$CD8^+$ T cells play a central role in antitumor immunity, and numerous studies have reported better outcomes in CRC cases with high expression of $CD8^+$ TILs (Yin et al., 2022; Williams et al., 2024). $CD4^+$ T cells encompass various functional subsets such as Th1, Th2, and Treg cells, and a general reduction in $CD4^+$ infiltration may reflect the suppression of antitumor subsets (e.g., Th1 cells) or the involvement of T cell exclusion mechanisms within the TME (Tosolini et al., 2011). Therefore, the reduction in $CD4^+$ and $CD8^+$ T cells along with low TIL scores observed in the high *KCNJ14* expression group may serve as potential biological indicators of resistance to immunotherapy. In contrast, no significant association was found between *KCNJ14* expression and infiltration of $FOXP3^+$ cells (mainly Tregs). This suggests that *KCNJ14*-mediated immunosuppression is likely independent of Treg involvement and may instead be driven by selective inhibition of $CD4^+$ and $CD8^+$ infiltration and altered chemokine dynamics leading to T cell exclusion.

Previous studies have shown that high *KCNJ14* expression is associated with activation of the mTOR pathway, vascular endothelial growth factor signaling, NOD-like receptor signaling, and increased expression of immune checkpoint molecules such as PD-L1 and CTLA-4 (Alasiri, 2023; Li et al., 2022). These pathways may contribute to the immunosuppressive phenotype observed in the TME. Future functional studies are warranted to determine whether *KCNJ14* directly modulates $CD4^+$ and $CD8^+$ T cell infiltration or activation via these molecular pathways. Although *KCNJ14* expression was not an independent prognostic factor for OS or RFS in our survival analysis, its consistent association with reduced immune infiltration and aggressive pathological features strongly suggests that *KCNJ14* expression plays a role in shaping the TME and influencing tumor responsiveness to immunotherapy.

Although recurrent genetic alterations of *KCNJ14* have not been reported in CRC, its overexpression is likely to be regulated at the transcriptional or epigenetic level rather than by direct genomic changes. One of the key strengths of the present study is the direct

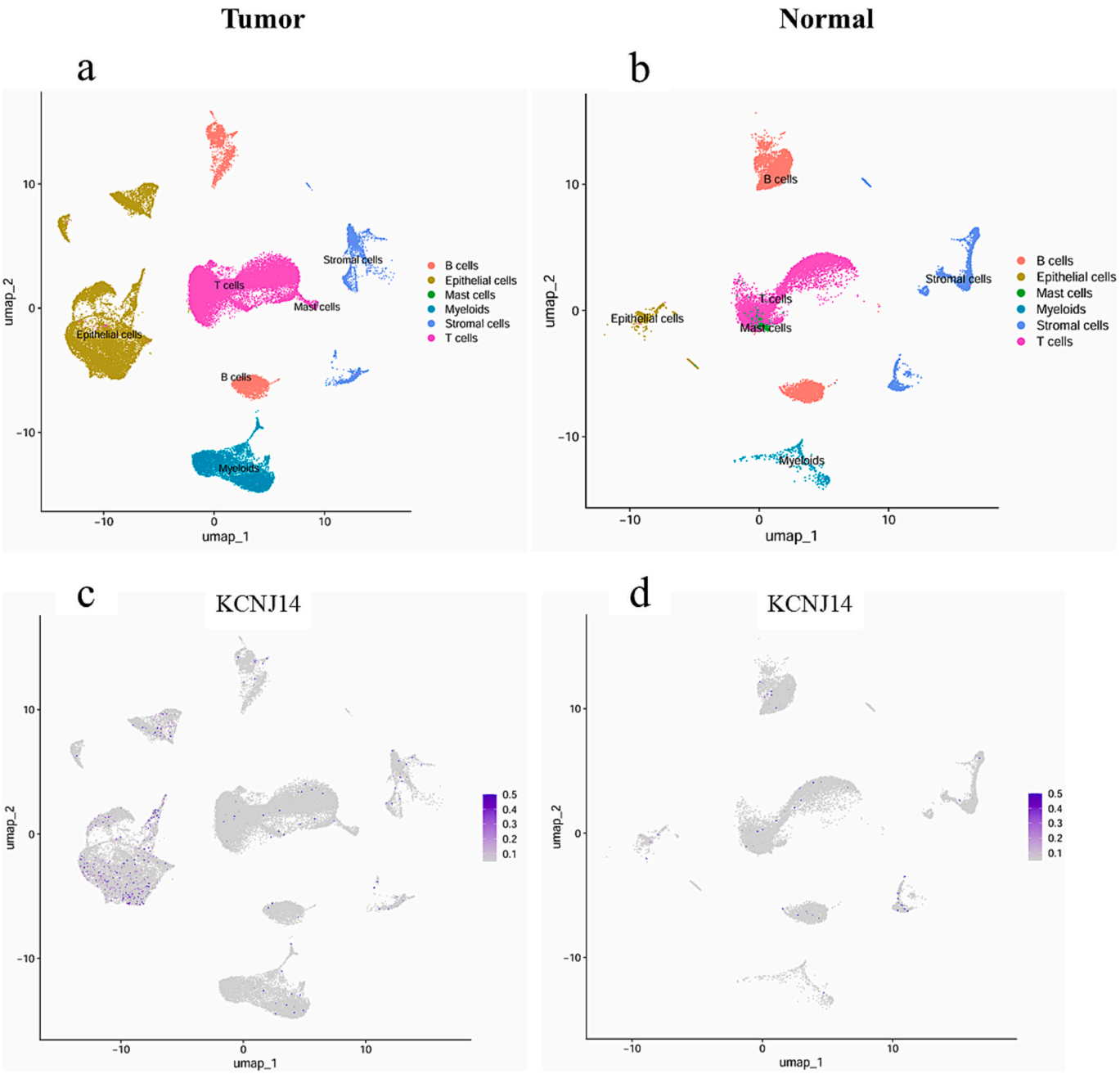

Fig. 7. Distribution of *KCNJ14* expression revealed by scRNA-seq analysis
Uniform manifold approximation and projection analysis using the publicly available scRNA-seq dataset visualized major cell populations in (a) CRC tissue and (b) normal colonic tissue. "Epithelial cells" in (a) refers to "cancer epithelial cells". (c) *KCNJ14* expression is predominantly observed in epithelial cell clusters within tumor tissues. (d) There is little to no *KCNJ14* expression in normal tissues. These results indicate that *KCNJ14* is selectively expressed in cancer cells in CRC, consistent with the findings from the RNA-ISH analysis.

visualization and quantification of *KCNJ14* mRNA expression at the cellular level using RNA-ISH, enabling spatially resolved analysis that is not possible with bulk RNA-sEq. (Wang et al., 2012). This approach proved effective in clarifying the expression of *KCNJ14* in cancer cells. Additionally, we used publicly available scRNA-seq CRC data to confirm that *KCNJ14* expression was specifically localized to epithelial cell populations within tumors. The concordance between the spatial expression patterns observed via RNA-ISH and the cell type-specific expression profiles identified by scRNA-seq strengthens the validity of our findings and supports the tumor cell-specific expression of *KCNJ14*.

The present study has several limitations. First, it was a retrospective study conducted at a single institution, and some patients with advanced pathological features received adjuvant chemotherapy. These factors may have influenced survival outcomes and partly explain why high *KCNJ14* expression, although associated with aggressive pathological features, did not correlate with overall or recurrence-free survival in our cohort. Second, the follow-up period was relatively short in some patients, which may have limited the detection of long-term prognostic differences. Third, the evaluation of the tumor microenvironment was restricted to local immune cell infiltration at the invasive front using TMA samples, without assessing the full spatial immune landscape of the tumor. Future studies should consider whole-slide imaging or spatial transcriptomic approaches. In addition, protein-level validation of *KCNJ14* could not be performed due to the lack of reliable antibodies for

FFPE tissues, and this remains an important direction for future studies. Finally, *KCNJ14* RNA-ISH scores in our cohort were distributed toward the lower end overall, and a threshold of $\geq 2+$ was adopted to define high expression. This criterion was based on the limited number of cases with high transcript levels; however, public datasets such as the Human Protein Atlas also report relatively low expression levels in colorectal tissue, which is consistent with our observations (Atlas, 2025). Compared with established markers such as Ki-67, which primarily reflects proliferative activity, *KCNJ14* may provide complementary prognostic information by integrating pathological aggressiveness with an immunosuppressive tumor microenvironment. Thus, *KCNJ14* should not be regarded as a redundant marker but rather as one that captures a different biological aspect of colorectal cancer behavior. Further validation in multicenter cohorts with longer follow-up is warranted.

5. Conclusions

This study is the first to use RNA-ISH on a CRC TMA to demonstrate that high *KCNJ14* expression is associated with reduced infiltration of $CD4^+$ and $CD8^+$ T cells and lower TIL scores. These findings suggest that *KCNJ14* may contribute to tumor progression and the establishment of an immunosuppressive TME, particularly a T cell-excluded phenotype of CRC. *KCNJ14* may serve as a clinically relevant biomarker for immunotherapy resistance and may be a potential therapeutic target. Further research is warranted to elucidate the underlying molecular mechanisms and explore the utility of *KCNJ14* in clinical applications.

List of abbreviations

CRC	colorectal carcinoma
dMMR	deficient mismatch repair
FFPE	formalin-fixed paraffin-embedded
H&E	hematoxylin and eosin
HPF	high-power field
IHC	immunohistochemistry
ISH	in situ hybridization
mTOR	mechanistic target of rapamycin
MSI	microsatellite instability
OS	overall survival
RFS	recurrence-free survival
RNA-ISH	RNA in situ hybridization
scRNA-seq	single-cell RNA sequencing
TIL	tumor-infiltrating lymphocytes
TMA	tissue microarray
TME	tumor microenvironment

CRediT authorship contribution statement

Hiroshi Sawaguchi: Writing – original draft, Validation, Methodology, Investigation, Conceptualization. **Takeshi Uehara:** Supervision, Funding acquisition, Conceptualization. **Mai Iwaya:** Validation. **Shiho Asaka:** Formal analysis. **Tomoyuki Nakajima:** Visualization, Validation, Formal analysis. **Shotaro Komamura:** Visualization, Validation, Formal analysis. **Shunsuke Imamura:** Conceptualization. **Yugo Iwaya:** Supervision, Methodology. **Shinsuke Sugenoya:** Resources. **Masato Kitazawa:** Investigation, Conceptualization. **Yuji Soejima:** Supervision, Methodology. **Hiroyoshi Ota:** Supervision, Data curation. **Tadanobu Nagaya:** Supervision, Methodology.

Ethics statement

The ethics committee of Shinshu University School of Medicine approved this study (approval code: 5836) and waived the requirement for informed consent. An opt-out method was used because of the retrospective design of the study. Information about the study was disclosed on the institutional website, and patients who declined participation were excluded. The investigation was conducted in compliance with the Declaration of Helsinki.

Funding

This research did not receive any specific grant from funding agencies in the public, commercial, or not-for-profit sectors.

Declaration of competing interest

The authors declare no competing interests.

Acknowledgements

We thank Masanobu Momose, Yasuyo Shimojo, Chitose Arai, Kanade Wakabayashi, Naoko Yamaoka, Saki Mukai, Daiki Ogura, Daiki Gomyo, and Tsukane Seki at Shinshu University Hospital for their excellent technical assistance. We also thank Kelly Zammit, BVSc, from Edanz (https://jp.edanz.com/ac) for editing a draft of this manuscript.

Data availability

All data generated and analyzed during the current study are available from the corresponding author on reasonable request.

References

Alasiri, G., 2023. Comprehensive analysis of KCNJ14 potassium channel as a biomarker for cancer progression and development. Int. J. Mol. Sci. 24.
Arnold, M., Sierra, M.S., Laversanne, M., Soerjomataram, I., Jemal, A., Bray, F., 2017. Global patterns and trends in colorectal cancer incidence and mortality. Gut 66, 683–691.
Atlas, H.P., 2025. KCNJ14 Expression in colon – The Human Protein Atlas.
Bray, F., Laversanne, M., Sung, H., Ferlay, J., Siegel, R.L., Soerjomataram, I., Jemal, A., 2024. Global cancer statistics 2022: GLOBOCAN estimates of incidence and mortality worldwide for 36 cancers in 185 countries. CA Cancer J. Clin. 74, 229–263.
Brierley, J.D.G.M., Wittekind, C., 2017. TNM Classification of Malignant Tumours. John Wiley & Sons.
Chiang, C.Y., Ching, Y.H., Chang, T.Y., Hu, L.S., Yong, Y.S., Keak, P.Y., Mustika, I., Lin, M.D., Liao, B.Y., 2020. Novel eye genes systematically discovered through an integrated analysis of mouse transcriptomes and phenome. Comput. Struct. Biotechnol. J. 18, 73–82.
Dienstmann, R., Vermeulen, L., Guinney, J., Kopetz, S., Tejpar, S., Tabernero, J., 2017. Consensus molecular subtypes and the evolution of precision medicine in colorectal cancer. Nat. Rev. Cancer 17, 79–92.
Fleming, M., Ravula, S., Tatishchev, S.F., Wang, H.L., 2012. Colorectal carcinoma: pathologic aspects. J. Gastrointest Oncol. 3, 153–173.
Hazra, R., Guo, J.D., Ryan, S.J., Jasnow, A.M., Dabrowska, J., Rainnie, D.G., 2011. A transcriptomic analysis of type I-III neurons in the bed nucleus of the stria terminalis. Mol. Cell. Neurosci. 46, 699–709.
Hernandez-Resendiz, I., Hartung, F., Pardo, L.A., 2019. Antibodies targeting K(V) potassium channels: a promising treatment for cancer. Bioelectricity 1, 180–187.
Jin, W., Lu, Y., Lu, J., Wang, Z., Yan, Y., Liang, B., Qian, S., Ni, J., Yang, Y., Huang, S., Han, C., Yang, H., 2025. Identification of cancer-associated fibroblast signature genes for prognostic prediction in colorectal cancer. Front. Genet. 16, 1476092.
Li, B., Ge, N., Pan, Z., Hou, C., Xie, K., Wang, D., Liu, J., Wan, J., Deng, F., Li, M., Luo, S., 2022. KCNJ14 knockdown significantly inhibited the proliferation and migration of colorectal cells. BMC Med. Genet. 15, 194.
Liu, J.L., Yang, M., Bai, J.G., Liu, Z., Wang, X.S., 2023. "Cold" colorectal cancer faces a bottleneck in immunotherapy. World J. Gastrointest. Oncol. 15, 240–250.
Nagtegaal, I.D.A.M.O.R., Lam, A.K., 2020. Tumours of the colon and rectum. In: o, ed (Ed.), WHO Classification of Tumours: Digestive System Tumours. International Agency for Research on Cancer (IARC), Lyon.
Nakajima, T., Uehara, T., Iwaya, M., Kobayashi, Y., Maruyama, Y., Ota, H., 2020. Characterization of LGR5 expression in poorly differentiated colorectal carcinoma with mismatch repair protein deficiency. BMC Cancer 20, 319.
Pardo, L.A., Stuhmer, W., 2014. The roles of K(+) channels in cancer. Nat. Rev. Cancer 14, 39–48.
Ropponen, K.M., Eskelinen, M.J., Lipponen, P.K., Alhava, E., Kosma, V.M., 1997. Prognostic value of tumour-infiltrating lymphocytes (TILs) in colorectal cancer. J. Pathol. 182, 318–324.
Siegel, R.L., Giaquinto, A.N., Jemal, A., 2024. Cancer statistics, 2024. CA Cancer J. Clin. 74, 12–49.
Topert, C., Doring, F., Wischmeyer, E., Karschin, C., Brockhaus, J., Ballanyi, K., Derst, C., Karschin, A., 1998. Kir2.4: a novel K+ inward rectifier channel associated with motoneurons of cranial nerve nuclei. J. Neurosci. 18, 4096–4105.

Topert, C., Doring, F., Derst, C., Daut, J., Grzeschik, K.H., Karschin, A., 2000. Cloning, structure and assignment to chromosome 19q13 of the human Kir2.4 inwardly rectifying potassium channel gene (KCNJ14). Mamm. Genome 11, 247–249.
Tosolini, M., Kirilovsky, A., Mlecnik, B., Fredriksen, T., Mauger, S., Bindea, G., Berger, A., Bruneval, P., Fridman, W.H., Pages, F., Galon, J., 2011. Clinical impact of different classes of infiltrating T cytotoxic and helper cells (Th1, th2, treg, th17) in patients with colorectal cancer. Cancer Res. 71, 1263–1271.
Ukpo, O.C., Flanagan, J.J., Ma, X.J., Luo, Y., Thorstad, W.L., Lewis Jr., J.S., 2011. High-risk human papillomavirus E6/E7 mRNA detection by a novel in situ hybridization assay strongly correlates with p16 expression and patient outcomes in oropharyngeal squamous cell carcinoma. Am. J. Surg. Pathol. 35, 1343–1350.
Wang, F., Flanagan, J., Su, N., Wang, L.C., Bui, S., Nielson, A., Wu, X., Vo, H.T., Ma, X.J., Luo, Y., 2012. RNAscope: a novel in situ RNA analysis platform for formalin-fixed, paraffin-embedded tissues. J. Mol. Diagn. 14, 22–29.
Williams, C.J.M., Gray, R., Hills, R.K., Shires, M., Zhang, L., Zhao, Z., Gardner, T., Sapanara, N., Xu, X.M., Bai, I., Yan, D., Muranyi, A., Dance, S., Aghaei, F., Hemmings, G., Hale, M., Kurkure, U., Guetter, C., Richman, S.D., Hutchins, G., Seligmann, J.F., West, N.P., Singh, S., Shanmugam, K., Quirke, P., 2024. Evaluation of CD3 and CD8 T-cell immunohistochemistry for prognostication and prediction of benefit from adjuvant chemotherapy in early-stage colorectal Cancer within the QUASAR trial. J. Clin. Oncol. 42, 3430–3442.
Wu, B., Zhang, B., Li, B., Wu, H., Jiang, M., 2024. Cold and hot tumors: from molecular mechanisms to targeted therapy. Signal Transduct. Target. Ther. 9, 274.
Yin, C., Okugawa, Y., Yamamoto, A., Kitajima, T., Shimura, T., Kawamura, M., Tsujiura, M., Okita, Y., Ohi, M., Toiyama, Y., 2022. Prognostic significance of CD8(+) tumor-infiltrating lymphocytes and CD66b(+) tumor-associated neutrophils in the invasive margins of stages I-III colorectal cancer. Oncol. Lett. 24, 212.
Zhang, J., Han, J., Li, L., Zhang, Q., Feng, Y., Jiang, Y., Deng, F., Zhang, Y., Wu, Q., Chen, B., Hu, J., 2021. Inwardly rectifying potassium channel 5.1: structure, function, and possible roles in diseases. Genes Dis 8, 272–278.
Zuniga, L., Cayo, A., Gonzalez, W., Vilos, C., Zuniga, R., 2022. Potassium channels as a target for Cancer therapy: current perspectives. Onco Targets Ther 15, 783–797.